

PAX2 re-expression in renal tubular epithelial cells and correlation with renal interstitial fibrosis of rats with obstructive nephropathy

Li Li, Yubin Wu & Weiguo Zhang

To cite this article: Li Li, Yubin Wu & Weiguo Zhang (2010) PAX2 re-expression in renal tubular epithelial cells and correlation with renal interstitial fibrosis of rats with obstructive nephropathy, Renal Failure, 32:5, 603-611, DOI: [10.3109/08860221003778049](https://doi.org/10.3109/08860221003778049)

To link to this article: <https://doi.org/10.3109/08860221003778049>



Published online: 20 May 2010.



Submit your article to this journal [↗](#)



Article views: 724



View related articles [↗](#)

LABORATORY STUDY

PAX2 re-expression in renal tubular epithelial cells and correlation with renal interstitial fibrosis of rats with obstructive nephropathy

Li Li¹, Yubin Wu¹ and Weiguo Zhang²

¹ Department of Pediatric Nephrology, Shengjing Hospital, China Medical University, Shenyang, China

² Cardiovascular and Neurological Consulting Institute, Irving, Texas, USA

ABSTRACT

Objective: To investigate the effect of paired box 2 (*PAX2*) gene re-expression in renal tubular epithelial cells on renal interstitial fibrosis in rats with obstructive nephropathy. **Methods:** Wistar rats were randomly divided into two groups: sham-operated group (sham group) and unilateral ureteral obstruction group (UUO group), 40 in each group. After the surgery, rats were killed at 3, 5, 7, and 14 days ($n = 10$ each) to remove and collect kidneys. Morphological changes of the kidney were determined by histopathology. Protein and mRNA expression of *PAX2* in the kidney were determined by immunohistochemistry, Western blot and real-time polymerase chain reaction (PCR). **Results:** The new major findings of this study include the following: (1) Hematoxylin and Eosin (HE) and Masson staining revealed obvious renal interstitial fibrosis in UUO group; (2) increased *PAX2* expression was found in renal tubular epithelial cells in UUO group by immunohistochemistry, but not in sham group; (3) by Western blot, a significant increase in *PAX2* protein level in UUO group was detected 3d after the surgery when compared to sham group ($p < 0.05$), which continued to increase with prolonged obstruction; the same pattern was also found in *PAX2* mRNA expression by real-time PCR in UUO group after the surgery; (4) *PAX2* protein level was positively correlated with the severity of renal tubular damage ($r = 0.937$ and $p < 0.05$) and the level of renal interstitial fibrosis ($r = 0.987$ and $p < 0.05$). **Conclusion:** In rats with obstructive nephropathy, embryonic development gene *PAX2* is re-expressed in the renal tubules, which may participate in the pathogenesis of renal tubular damage and renal interstitial fibrosis.

Keywords: renal tubule epithelial cells; interstitial fibrosis; *PAX2*; UUO; chronic kidney disease

Received 13 December 2009; revised 21 January 2010; accepted 7 February 2010

Correspondence: Prof. Yubin Wu, Department of Pediatric Nephrology, Shengjing Hospital, China Medical University, No. 36 Sanhao Street, Heping District, Shenyang 110004, China; tel: 96615-56211; fax: 96615-13631; E-mail: wuyb@sj-hospital.org

INTRODUCTION

Obstructive nephropathy is a clinical syndrome resulting from structural and (or) functional changes of urinary tract that impede urination, leading to renal pathological changes and dysfunction. The major pathological characteristics of obstructive nephropathy include renal tubular atrophy and interstitial fibrosis, with epithelial–mesenchymal transition (EMT) being one of the important pathogenic mechanisms of renal interstitial fibrosis.^{1,2} Obstructive nephropathy is the primary cause for end-stage renal disease (ESRD) in infants and children, which represents 16.1% of all pediatric transplantations in North America. The overall prevalence of obstructive nephropathy is 0.3% in ESRD patients in North American population.³ Therefore, it is of great financial and social significance to delay, prevent, or even reverse the progress of renal damage caused by obstructive nephropathy.

Paired box 2 (*PAX2*) gene encodes a nuclear transcription factor, a key gene to induce the renal tubular epithelial cell transition during embryonic development. It is involved in the regulation of embryonic development of kidney at various stages.⁴ Its expression is turned off in mature nephrons. It was found in recent years⁵ that *PAX2* gene was expressed at different levels in renal tubular epithelial cells in children with glomerular diseases, suggesting that restoration of *PAX2* may lead to renal tubular epithelial cell transdifferentiation. Cohen et al.⁶ found that in unilateral ureteral obstruction (UUO) model, reactivation of *PAX2* was noted primarily in collecting ducts of the obstructed kidney, indicating its role in inhibiting collecting duct cell apoptosis and reducing renal parenchyma damage. However, the effect of *PAX2* re-expression on renal interstitial fibrosis in UUO kidney has not been determined yet. In this study, by establishing an obstructive nephropathy model with unilateral ureteral ligation, we explored the dynamic changes of

PAX2 gene in obstructive nephropathy and its correlation with renal interstitial fibrosis to provide experimental evidences for the potential role of *PAX2* in the prevention and treatment of renal interstitial fibrosis.

MATERIAL AND METHODS

Model preparation and grouping

Wistar rats (120–150 g) were obtained from the Laboratory Animal Center of Shengjing Hospital, China Medical University (Shenyang, China), and maintained in sterile cages under specific pathogen-free conditions. Animals were randomly divided into sham-operated group and UUO group, $n = 40$ each. To establish UUO model, rats in UUO group were anesthetized by intraperitoneal injection of 10% chloral hydrate (300 mg/kg), the left kidney and ureter were exposed via a flank incision. Left ureter was identified along the inferior pole of left kidney, which was then ligated at both proximal and distal points using 4–0 silk suture. Ureter was severed between these two ligation points. In sham group, ureter was isolated but not ligated. The abdominal cavity was then closed in layers. Rats were killed at 3, 5, 7, and 14 days after surgery (10 in each group at each time point).

Tissue preparation

Under same anesthesia, kidneys were taken out. A small portion of the renal tissue was taken and fixed in 4% paraformaldehyde for pathomorphology and immunohistochemical assays. Surface fatty tissue was detached and renal cortex was separated from medulla. Then the renal tissues were wrapped in sterile aluminum foil, flash-frozen by liquid nitrogen, and stored at -80°C for real-time fluorescence quantitative polymerase chain reaction (PCR) and Western blot assay.

Pathomorphology observation and evaluation

Renal tubular damage extent

Renal tissue was embedded in paraffin and was stained with standard HE method. Under light microscopy tubulointerstitial damage was assessed.⁷ Each of three parameters of tubulointerstitial damage (i.e., tubule proteinaceous casts and dilation, interstitial inflammation, interstitial fibrosis) was assigned a score from 0 to 3 according to severity (0 = no abnormality, 1 = mild, 2 = moderate, 3 = severe), and these scores were added to yield an overall tubulointerstitial score from 0 to 9 (arbitrary units). The pathologist, who read and scored the tissue damage, was unaware of the group assignment of individual rat.

Renal interstitial fibrosis

Fibrosis was assessed by measuring collagen deposition in Masson's trichrome stained slides according to the standard protocol (Fujian Maxim Company, Fujian, China). In each section with Masson's trichrome staining, 10 fields were digitized and scanned at $400\times$ magnification by using NIS-Elements BR 2.10 image analysis software (Nikon, Tokyo, Japan). Using a grid superimposed on the image, the number of blue collagen staining points was counted, and the percentage of blue collagen area in the examined tubulointerstitial was measured.⁸ Average of this ratio represented relative area of renal interstitium on each slide.

Analysis of *PAX2* protein expression

Immunohistochemistry

Tissues fixed in 4% (w/v) formalin were dehydrated in graded alcohol and embedded in paraffin. Sections ($5\ \mu\text{m}$ in thickness) were prepared and subjected to the immunoperoxidase method. Endogenous peroxidase was eliminated by treatment with 3% H_2O_2 for 10 min at room temperature. After washing with water and 0.02 M phosphate-buffered saline (PBS) (pH 7.4), slides were incubated with 5% bovine serum albumin (BSA) in PBS for 10 min at room temperature to prevent non-specific protein binding and then with primary rabbit antibodies to *PAX2* (5 $\mu\text{g}/\text{mL}$; Zymed, South San Francisco, CA, USA) at 4°C overnight. The sections were washed in PBS and then incubated for 20 min in biotinylated secondary antibody with avidin-tagged horseradish peroxidase (Fujian Maxim Company) at room temperature. Immunoreactive *PAX2* was identified with diaminobenzidine (DAB) peroxidase substrate kit (Beijing Zhongshan Biotechnology Company, Beijing, China) and counterstained with hematoxylin (Fujian Maxim Company). For the negative control, slides were processed without incubating with primary antibody. The optical densities per unit area of *PAX2* were determined by densitometric scanning using a NIS-Elements F 2.30 image acquisition software and NIS-Elements BR 2.10 image analysis software. The value of the optical density of each protein was expressed as mean \pm SD.

Western blotting

Kidneys were homogenized in lysis buffer (Shanghai JiKai Company, Shanghai, China). Loading dye was added and the samples were boiled at 100°C for 5 min, spun, and submitted to electrophoresis on a 10% polyacrylamide gel at 100V for 2 hours. Proteins were then transferred electrophoretically to polyvinylidene fluoride (PVDF) membrane for 1 hour at 80V. After electroblotting, the membranes were blocked with 5% dried skim milk in Tris-buffered saline with 0.05% Tween (TBS-T) overnight at 4°C , followed by incubation for 2 hours at room temperature with rabbit polyclonal *PAX2* antibody

(1 µg/mL). Then the membrane was washed with PBS-T and horseradish peroxidase-labeled goat anti-rabbit IgG (0.2 µg/mL; Santa Cruz Biotechnology, Santa Cruz, CA, USA) was added for 1 hour at room temperature. The blots were washed three times for 5 min in TBS-T, followed by incubation in DAB chromogenic solution. Semi-quantitative method was used to analyze *PAX2* expression in renal tissue, and protein bands on membrane were scanned and saved in computer. Quantity One-4.4.0 software system was used to analyze the optical density of protein bands. Intensities from the *PAX2* bands were divided by the β -actin band intensities to normalize the loading variation.

Real-time quantitative PCR to analyze *PAX2* mRNA expression

Total RNA was extracted from rats' renal cortex with TRIzol reagent (Invitrogen, Carlsbad, California, USA) according to the manufacturer's protocol. The yield and quality of the RNA were assessed by measuring the absorbance at 260 and 280 nm. Total RNA (500 ng) was reverse-transcribed into complementary DNA (cDNA) using the PrimeScript™ RT Reagent KIT (Takara, Otsu, Shiga, Japan) according to the manufacturer's guideline. Quantitative real-time PCR was performed for *PAX2* (mRNA: NM_001106361) and GAPDH using the following primer pairs (synthesized by Shanghai ShengGong Biotechnology Company, Shanghai, China): *PAX2* sense primer 5'-CGGTGAGAAGAGGAAACGAG-3' and antisense primer 5'-GCTTGGGAAGACATCGGGATA-3', GAPDH sense primer 5'-TGTGTCCGTCGTGGATCTGA-3' and antisense primer 5'-ATGGTGGTGAAGACG CCAAGTA-3'. A 20 µL PCR reaction solution (SYBR Premix Ex Taq™(2×) 10 µL; 10 µmol/L forward primer 0.4 µL; 10 µmol/L reverse primer 0.4 µL; cDNA 2 µL; ROX Reference Dye(50×) 0.4 µL; dH₂O 6.8 µL) was amplified in ABI 7500 real-time PCR system (Applied Biosystems, Foster City, CA, USA) with the following thermal cycling conditions: 1 cycle at 95°C for 10 s, followed by 40 cycles at 95°C for 5 s and 60°C for 34 s, which can spontaneously show the results according to the standard curve. The sample with the largest Ct value in pre-test was used as the standard to each gene and diluted into four gradients with EAZY Dilution, constructing the standard curve. All the samples were amplified at the same time and run in triplicates. The gene signals were standardized against the corresponding GAPDH signal, and results were expressed as the ratio of each molecule to GAPDH. Relative levels of mRNA expression were carried out using the standard curve method.

Statistical analysis

Experimental data were shown as mean ± SD. SPSS13.0 software was used for statistical analysis.

Inter-group comparison was done by *t*-test, intra-group comparison was done by one-way analysis of variance (ANOVA), and correlation analysis between two variables was done by Pearson correlation analysis. *p* < 0.05 was considered as the statistical significance.

RESULTS

Morphological changes of renal tissue

Macroscopic observation

By gross anatomy, rat kidney of sham group was dark-red color with smooth surface intact renal capsule that was not attached to renal parenchyma and clear boundary between cortex and medulla.

On the contrary, rat kidney of UUO group was enlarged with prolonged obstruction and appeared as lackluster, rough surface, visible hydronephrosis, thinner renal parenchyma, dilated renal pelvis, compressed papilla, flat and blunt fornix papilla, some of which became concave shape (Figure 1).

Pathological changes of kidney under light microscope

HE staining showed that renal tubules of rats in sham group were compact and well organized. By contrast,

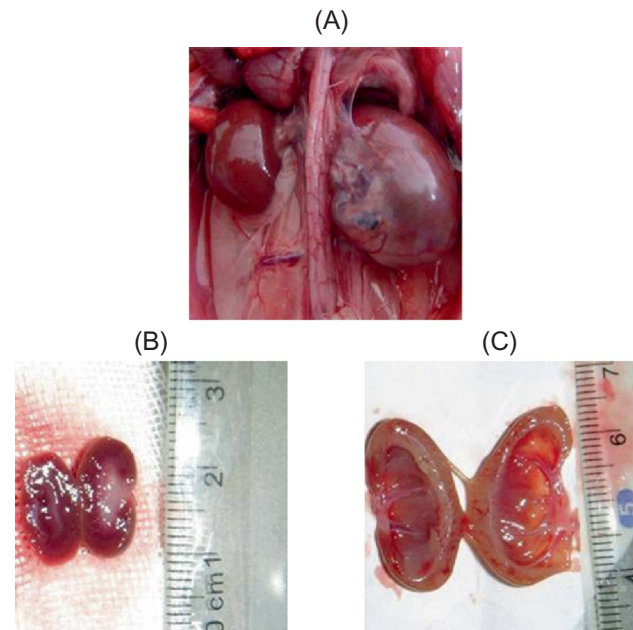


FIGURE 1. Gross anatomy of kidney. (A) At 14d after UUO, kidney was significantly enlarged. (B) In sham group, renal cortex and medulla had clear boundary. (C) Kidneys in UUO group showed obvious thinning of renal parenchyma, dilated renal pelvis, and compressed papilla and flattened and blunt fornix papilla, some of which turned into concave shape.

in rats from UUO group, renal interstitial edema was observed and renal tubules were dilated at 3d after the operation. Monocyte and lymphocyte infiltration appeared at tubulointerstitial region. Renal damage gradually worsened with prolonged obstruction. At 14d after the operation, renal tubular structure was severely damaged. Renal tubules became atrophic; renal tubules and collecting duct dilated into cystic shape. Tubular lumen collapsed and a large number of epithelial cells underwent necrosis. Diffusive infiltration of macrophage and lymphocyte appeared at renal interstitium, with obvious fibroblast hyperplasia and interstitial collagen deposition. However, no visible glomerular lesions were detected at different time points. There were significant differences in renal tubular damage scores between the sham and UUO groups ($p < 0.05$). Comparison among different time points of UUO group revealed $p < 0.05$ (Figure 2 and Table 1).

TABLE 1. Renal tubular damage score in each group (%), mean \pm SEM, $n = 10$).

	3d	5d	7d	14d
Sham	0.11 \pm 0.03	0.13 \pm 0.05	0.10 \pm 0.02	0.15 \pm 0.10
UUO	2.50 \pm 0.27*	3.72 \pm 0.61**	4.65 \pm 0.72**	6.12 \pm 0.89**

Note: * $p < 0.05$, compared to the sham group; ** $p < 0.05$, intra-group comparison in UUO group.

Masson staining showed, in sham group, renal collagen staining mainly located at tubular basement membrane, renal capsule, mesangial region, and area surrounding capillaries between renal tubules. Little staining was found around interstitium between renal tubules. In UUO group, at 3d after the operation, collagen deposition was visible, which was progressively

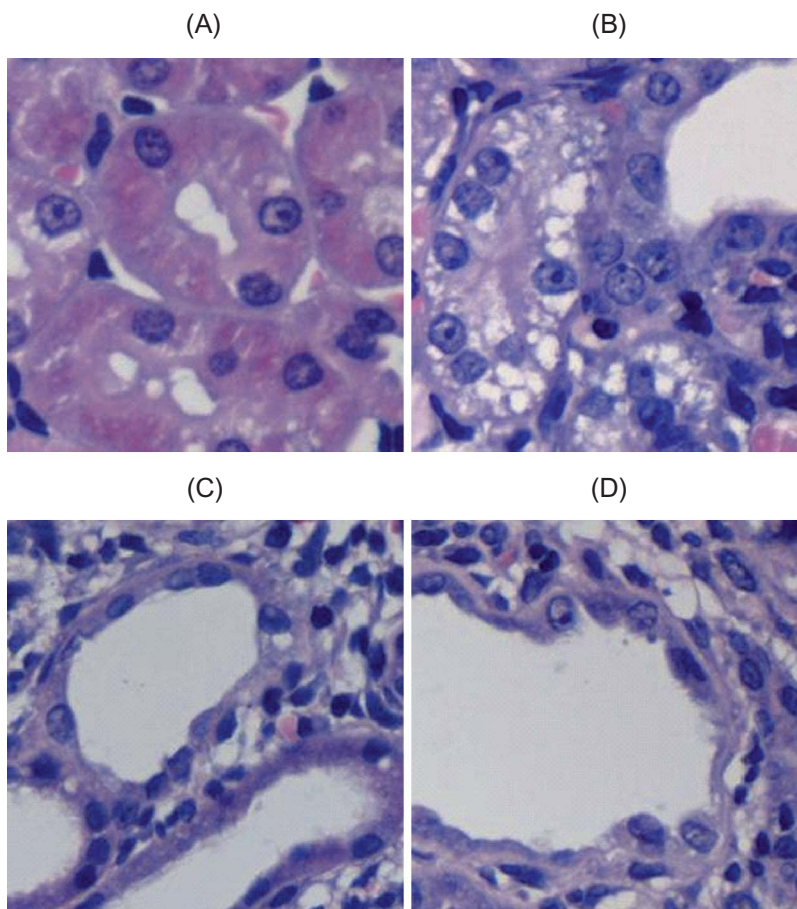


FIGURE 2. General pathological changes caused by UUO (HE staining). (A) No abnormal changes were detected in sham-operated rats. (B) At 3d after UUO, inflammatory cell infiltration and tubular edema appeared. (C) In UUO group, renal tubular dilation was observed at 7d after obstruction. Visible renal interstitial edema, monocyte and lymphocyte infiltration appeared at tubulointerstitial region. (D) In UUO group, renal tubular structure was severely damaged at 14d after obstruction, that is, collapsed lumen, diffusive infiltration of fibroblast in renal interstitium, and collagen formation. Original magnification $\times 400$.

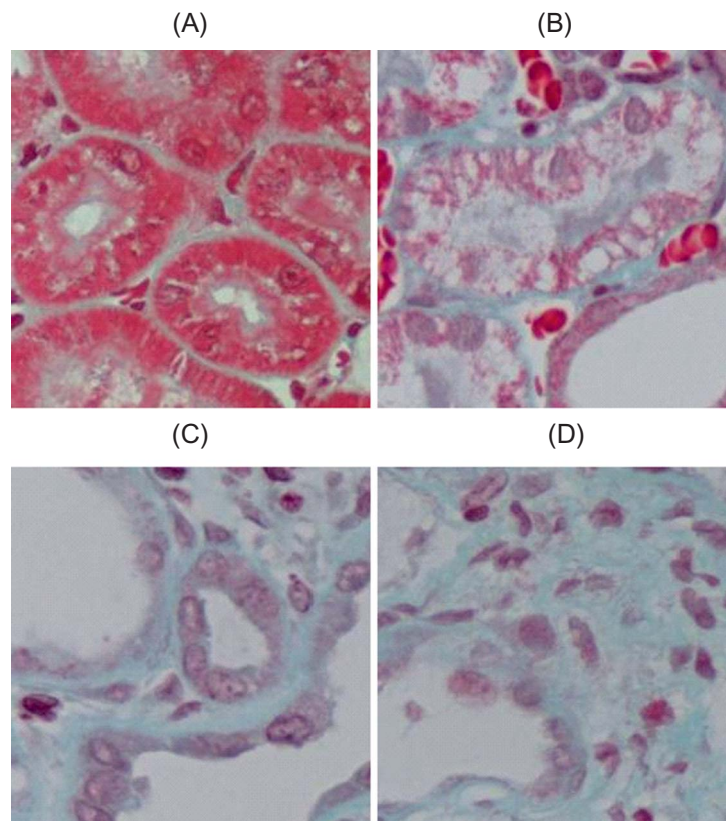


FIGURE 3. Collagen/fibrosis caused by UUO (Masson staining). (A) No abnormal changes were detected in sham-operated rats. (B) In UUO group, mild tubulointerstitial damage was noticed at 3d after obstruction. (C) At 7d after obstruction, UUO group showed renal interstitium widening and collagen deposition. (D) In UUO group, renal interstitial fibrosis significantly increased at 14d after obstruction, with increased extracellular matrix complexity and obvious collagen deposition. Original magnification $\times 400$.

TABLE 2. Relative area of renal interstitium in each group (% , mean \pm SEM, $n = 10$).

	3d	5d	7d	14d
Sham	1.77 \pm 0.23	1.57 \pm 0.31	1.65 \pm 0.72	1.89 \pm 0.30
UUO	7.31 \pm 1.03*	15.57 \pm 1.67**	23.27 \pm 2.17**	32.70 \pm 2.51**

Note: * $p < 0.05$, compared to the sham group; ** $p < 0.05$, intra-group comparison in UUO group.

increased with prolonged obstruction. Renal interstitium gradually widened, and mesenchymal cells and extracellular matrix complexity increased. Renal interstitial fibrosis relative area was significantly larger than that of the sham group ($p < 0.05$) (Figure 3 and Table 2).

Changes of *PAX2* protein expression in kidney in UUO rats

Immunohistochemistry showed that in sham group, *PAX2* protein had no expression in renal tubular epithelial cells, while relatively abundant expression was identified in nuclei of collecting duct epithelial cells. In

UUO group, *PAX2* protein expression appeared in renal tubular epithelial cells at 3d after the operation and became more apparent at 14d after the operation ($p < 0.05$). Expression level of *PAX2* was significantly higher than that of sham group ($p < 0.05$) (Figure 4).

Western blotting results showed that in the sham group, trace amount of *PAX2* protein was expressed at renal cortex, while increased *PAX2* protein expression was detected in UUO group at 3d after the operation, which rapidly increased with prolonged obstruction ($p < 0.05$). The relative protein expression level of *PAX2*/ β -actin in obstructive renal

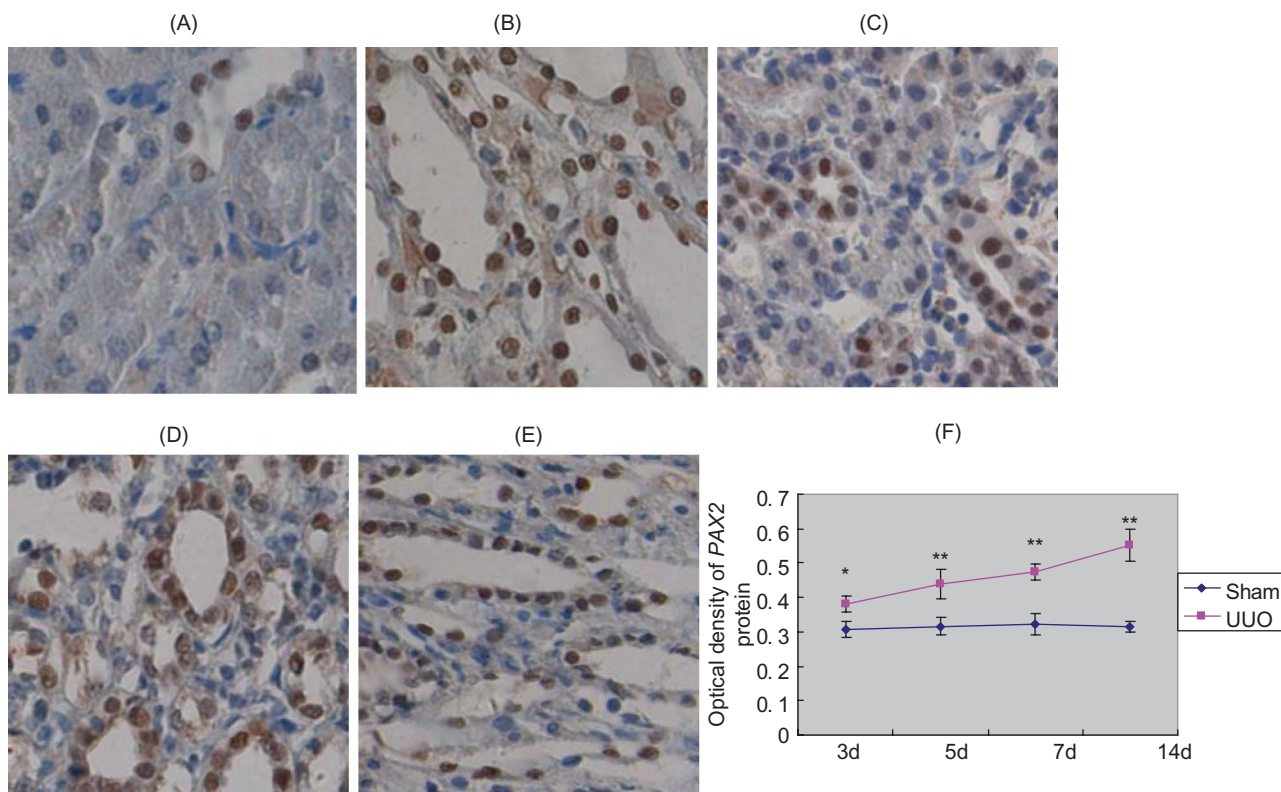


FIGURE 4. *PAX2* protein expression in rat renal tissues. In renal cortex of sham group, no *PAX2* expression was detected in renal tubular epithelial cells, *PAX2* expression was detected in collecting duct epithelial cells (A). In renal medulla of sham group, relative abundant *PAX2* expression was seen in collecting duct epithelial cells (B). At 3d after UUO, *PAX2* expression appeared in renal tubular epithelial cells and collecting duct epithelial cells (C). At 14d after obstruction, *PAX2* expression became more pronounced in renal tubular epithelial cells (D). At 14d after obstruction, *PAX2* expression was detected in collecting duct epithelial cells of renal medulla (E). Original magnification $\times 400$. In UUO group, average optical density of *PAX2* protein significantly increased with prolonged obstruction (F).

Note: * $p < 0.05$ compared to sham group; ** $p < 0.05$ for intra-group comparison in UUO group.

cortex was significantly higher than that of sham group ($p < 0.05$) (Figure 5).

***PAX2* mRNA expression**

Real-time quantitative PCR results showed that in sham group, trace amount of *PAX2* mRNA was expressed at renal cortex, while increased *PAX2* mRNA expression was detected in UUO group at 3d after the surgery, which rapidly increased with prolonged obstruction ($p < 0.05$). Relative gene copy number of *PAX2* mRNA/GAPDH mRNA was significantly different between these two groups ($p < 0.05$) (Figure 6).

Correlation analysis

We performed Pearson correlation analysis on *PAX2* protein expression level, renal tubular damage score, and relative area of renal interstitium. Results showed that *PAX2* protein level was positively correlated with the severity of renal tubular damage ($r = 0.937$

and $p < 0.05$) and the level of renal interstitial fibrosis ($r = 0.987$ and $p < 0.05$).

DISCUSSION

Urinary tract obstruction results in obstructive nephropathy. It is the most frequent cause of renal failure in infants and children.⁹ Renal interstitial fibrosis is the common final pathway for all obstructive nephropathies. Experimentally, UUO is the most classic animal model for inducing renal fibrosis,^{10,11} because it is simple and reproducible. In this study, both HE staining and Masson staining showed obvious renal fibrosis characteristics such as inflammatory cell infiltration, renal tubular and interstitial changes, and interstitial collagen deposition, indicating the successful establishment of UUO model.

PAX2 gene encodes a nuclear transcription factor and plays a pivotal role for embryonic kidney

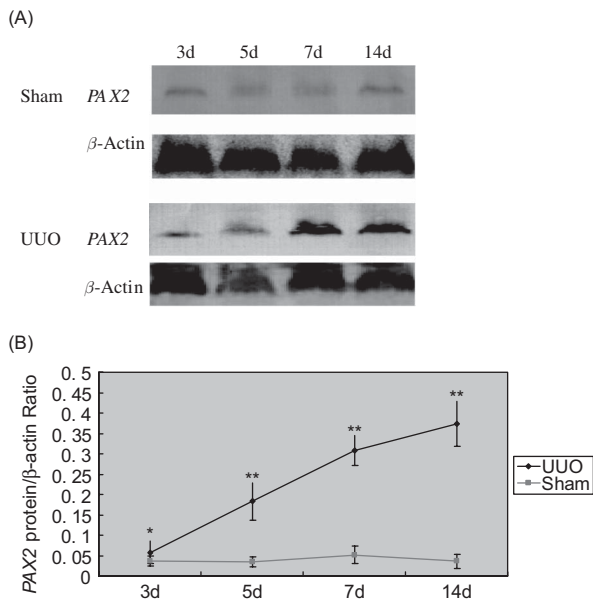


FIGURE 5. Western blotting analysis of *PAX2* protein expression. (A) The expression of *PAX2* and β -actin proteins in UUO and sham groups. (B) The ratio of *PAX2* and β -actin proteins in UUO and sham groups. Note: * $p < 0.05$ compared to sham group; ** $p < 0.05$ for intra-group comparison in UUO group.

development.¹² It is expressed during the entire developmental process of pronephron, mesonephron, and metanephron, involving the regulation of embryonic kidney development at various fetal stages,⁴ but its expression disappeared in mature nephrons.¹³ During normal kidney development, interactions between the arborizing ureteric bud (UB) and the metanephric mesenchyme (MM) generate the nephrons of each kidney. As a “kidney-specific” master gene, *PAX2* is expressed in both UB and MM lineages, normally optimizing UB branching and mesenchymal-to-epithelial transformation (MET) in kidney development. *PAX2* is involved both in the process whereby MM is transformed into polarized epithelium and/or in the maturation of the proximal convoluted tubule as it undergoes terminal differentiation.^{14,15} When *PAX2* gene was mutated, MET was consequently blocked, indicating that *PAX2* plays an important role in regulating the mesenchymal–epithelial trans-differentiation.¹⁶

Recently, it was found that *PAX2* was re-expressed in nephropathy.¹⁷ In immune kidney diseases, Letavernier et al.¹⁸ observed changes in podocyte phenotypes in focal segmental glomerulosclerosis (FSGS), including de-differentiation of podocytes, in

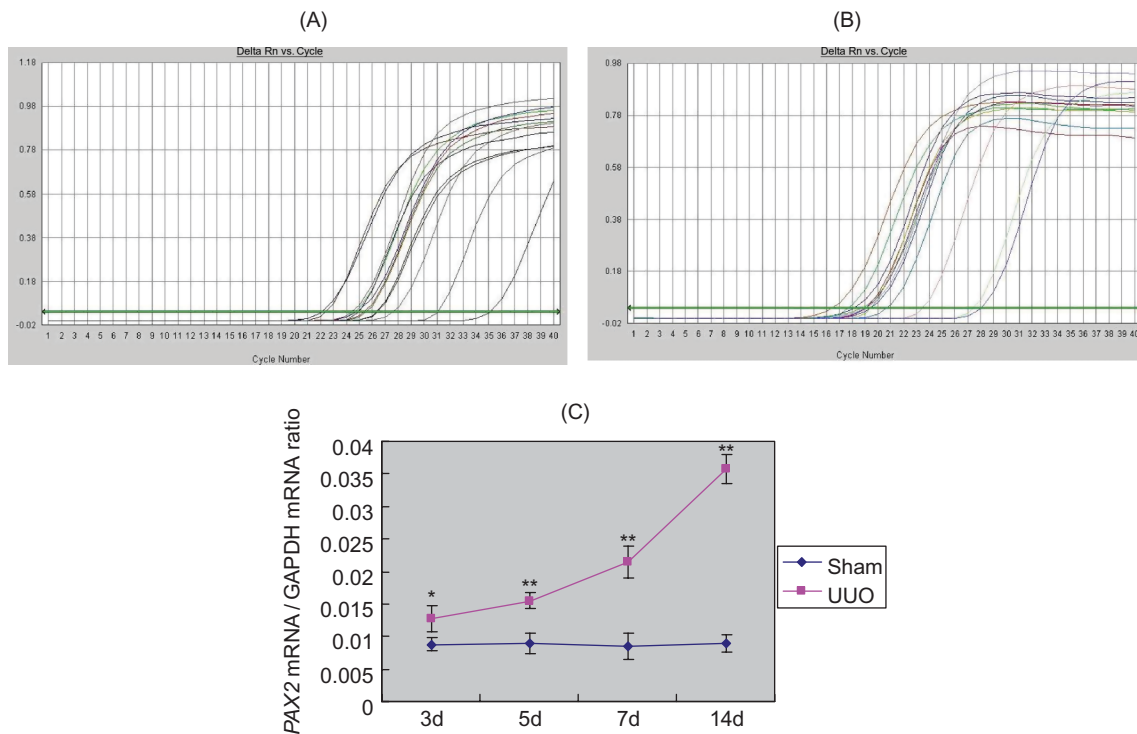


FIGURE 6. Real-time quantitative PCR analysis of *PAX2* mRNA expression. (A) Amplification curve of *PAX2*. (B) Amplification curve of GAPDH. (C) With prolonged obstruction, the ratio of *PAX2* mRNA/GAPDH mRNA significantly increased in UUO group. Note: * $p < 0.05$ compared to sham group; ** $p < 0.05$ for intra-group comparison in UUO group.

parallel to the expression of fetal *PAX2*, indicating that expression of *PAX2* might cause these changes in podocyte phenotypes. Phenotypic change of podocyte in the cellular lesion (CL) resembles MET. It is likely that re-expression of *PAX2* leads to a phenotypic change of the podocyte, which seems to be a developmental paradigm and may be responsible for the development of the CL in primary FSGS.¹⁹ *PAX* gene re-expression in terminally differentiated cells leads to cell de-differentiation,²⁰ which is related to the occurrence of podocyte pathology. Zhang et al.²¹ found that in primary nephrotic syndrome, *PAX2* expression in renal tubules in steroid-resistant children was significantly increased than that in steroid-sensitive children. The fact that the *PAX2* expression is positively correlated with renal damage suggests that *PAX2* re-expression may be one of the mechanisms for steroid resistance in childhood primary nephrotic syndrome.

In a study on nonimmune renal disease, Cohen et al.⁶ detected *PAX2* re-expression in renal collecting duct cells in UUO obstructive kidney model, while our results showed that *PAX2* re-expression was located at renal tubular epithelium. In addition, immunohistochemistry showed that no *PAX2* protein was expressed in renal tubular epithelial cells of the sham group, while relative abundant expression was detected in nuclei of the collecting duct epithelial cells. In UUO group, *PAX2* protein and mRNA were re-expressed in renal tubular epithelial cells at 3d after the operation, which became more pronounced with prolonged obstruction, and expressed at a significant level at 14d after the surgical operation. Furthermore, *PAX2* protein level, degrees of renal tubular damage, and renal fibrosis were positively correlated. During embryonic development, MET is an important physiological activity for the formation of kidney, while EMT is the reversed process of embryonic development.²² One of the critical steps of renal fibrosis is the reversal of embryonic development. In other words, the inherent renal epithelial cells acquired phenotypes of primitive embryonic mesenchyme, that is, renal tubular epithelial-myofibroblast transdifferentiation has been repeatedly proven to be dominant in the formation of renal fibrosis.^{23–27} Therefore, we believe that the re-expression of *PAX2* may be resulting from the initiation of renal fibrosis regulatory mechanisms, which activate the procedure of renal tubular epithelial cell transdifferentiation. In addition, renal tubular epithelial cells have a certain degree of plasticity in their morphology and function, so that *PAX2* re-expression may also be a protective response for tissue damage. When the micro-environment of embryonic development is restored, cell regeneration

after damage can be promoted and renal tubular epithelial cell transition can be reversed.

In summary, this study demonstrated that the fetal *PAX2* gene was re-expressed in rats with UUO, which were correlated with and likely to be causal for renal tubular damage and renal interstitial fibrosis. The specific molecular mechanisms and signaling pathway still need to be further investigated.

Acknowledgment

The authors are indebted to staff at Central Laboratory of China Medical University for their technical assistance.

Declaration of interest: The authors report no conflicts of interest. The authors alone are responsible for the content and writing of the paper.

REFERENCES

- [1] Zeisberg M, Kalluri R. The role of epithelial-to-mesenchymal transition in renal fibrosis. *J Mol Med.* 2004;82(3):175–181.
- [2] Liu Y. Renal fibrosis: New insights into the pathogenesis and therapeutics. *Kidney Int.* 2006;69(2):213–217.
- [3] Bascands JL, Schanstra JP. Obstructive nephropathy: Insights from genetically engineered animals. *Kidney Int.* 2005 Sep;68(3):925–937.
- [4] Narlis M, Grote D, Gaitan Y, Boualia SK, Bouchard M. *PAX2* and *Pax8* regulate branching morphogenesis and nephron differentiation in the developing kidney. *J Am Soc Nephrol.* 2007;18(4):1121–1129.
- [5] Geng WM, Yi ZW, He XJ, et al. Function of *PAX2* in tubular epithelium transdifferentiation. *J Clin Pediatr.* 2007;25(4): 284–287.
- [6] Cohen T, Loutochin O, Amin M, Capolicchio JP, Goodyer P, Jednak R. *PAX2* is reactivated in urinary tract obstruction and partially protects collecting duct cells from programmed cell death. *Am J Physiol Renal Physiol.* 2007;292(4): F1267–F1273.
- [7] Taal MW, Zandi-Nejad K, Weening B, et al. Proinflammatory gene expression and macrophage recruitment in the rat remnant kidney. *Kidney Int.* 2000;58(4):1664–1676.
- [8] Mizuguchi Y, Miyajima A, Kosaka T, Asano T, Asano T, Hayakawa M. Atorvastatin ameliorates renal tissue damage in unilateral ureteral obstruction. *J Urol.* 2004;172(6 Pt 1):2456–2459.
- [9] Chen F. Genetic and developmental basis for urinary tract obstruction. *Pediatr Nephrol.* 2009;24(9):1621–1632.
- [10] Picard N, Baum O, Vogetseder A, Kaissling B, Le Hir M. Origin of renal myofibroblasts in the model of unilateral ureter obstruction in the rat. *Histochem Cell Biol.* 2008;130(1):141–155.
- [11] Kaneto H, Morrissey J, McCracken R, Reyes A, Klahr S. Enalapril reduces collagen type IV synthesis and expansion of the interstitium in the obstructed rat kidney. *Kidney Int.* 1994; 45(6):1637–1647.
- [12] Rothenpieler UW, Dressler GR. Pax-2 is required for mesenchyme-to-epithelium conversion during kidney development. *Development.* 1993;119(3):711–720.
- [13] Eccles MR, Wallis LJ, Fidler AE, Spurr NK, Goodfellow PJ, Reeve AE. Expression of the *PAX2* gene in human fetal kidney and Wilms' tumor. *Cell Growth Differ.* 1992;3(5): 279–289.
- [14] Grote D, Souabni A, Busslinger M, Bouchard M. Pax-2/8-regulated Gata 3 expression is necessary for morphogenesis and guidance of the nephric duct in the developing kidney. *Development.* 2006;133(1):53–61.

- [15] Torban E, Dziarmaga A, Iglesias D, et al. *PAX2* activates *WNT4* expression during mammalian kidney development. *J Biol Chem*. 2006;281(18):12705–1212.
- [16] Liu Y. Epithelial to mesenchymal transition in renal fibrogenesis: pathologic significance, molecular mechanism, and therapeutic intervention. *J Am Soc Nephrol*. 2004;15(1):1–12.
- [17] Fukuzawa R, Eccles M, Ikeda M, Hata J. Embryonal hyperplasia of Bowman's capsular epithelium in patients with *WT1* mutations. *Pediatr Nephrol*. 2003;18(1):9–13.
- [18] Letavernier E, Bruneval P, Mandet C, et al. High sirolimus levels may induce focal segmental glomerulosclerosis de novo. *Clin J Am Soc Nephrol*. 2007;2(2):326–333.
- [19] Ohtaka A, Ootaka T, Sato H, Ito S. Phenotypic change of glomerular podocytes in primary focal segmental glomerulosclerosis: Developmental paradigm? *Nephrol Dial Transplant*. 2002;17(Suppl. 9):11–15.
- [20] Wagner KD, Wagner N, Guo JK, et al. An inducible mouse model for *PAX2*-dependent glomerular disease: Insights into a complex pathogenesis. *Curr Biol*. 2006;16(8):793–800.
- [21] Zhang HQ, Yi ZW, He XJ, Dang XQ, He QN, Mo SH. *PAX2* expression in children with steroid-resistant primary nephrotic syndrome. *Zhong Nan Da Xue Xue Bao Yi Xue Ban*. 2005;30(5):597–600.
- [22] E1-Nahas AM. Plasticity of kidney cells: Role in kidney remodeling and scarring. *Kidney Int*. 2003;64(5):1553–1563.
- [23] Chevalier RL. Chronic partial ureteral obstruction and the developing kidney. *Pediatr Radiol*. 2008;38(Suppl. 1):S35–S40.
- [24] Wynn TA. Cellular and molecular mechanisms of fibrosis. *J Pathol*. 2008;214(2):199–210.
- [25] Li MX, Liu BC. Epithelial to mesenchymal transition in the progression of tubulointerstitial fibrosis. *Chin Med J (Engl)*. 2007;120(21):1925–1930.
- [26] Burns WC, Kantharidis P, Thomas MC. The role of tubular epithelial–mesenchymal transition in progressive kidney disease. *Cells Tissues Organs*. 2007;185(1–3):222–231.
- [27] Rastaldi MP. Epithelial–mesenchymal transition and its implications for the development of renal tubulointerstitial fibrosis. *J Nephrol*. 2006;19(4):407–412.